Pharm Res (2014) 31:3201–3210
DOI 10.1007/s11095-014-1412-5

RESEARCH PAPER

Pulsatile Protein Release from Monodisperse Liquid-Core Microcapsules of Controllable Shell Thickness

Yujie Xia • Daniel W. Pack

Received: 20 January 2014 / Accepted: 6 May 2014 / Published online: 16 May 2014

ABSTRACT

Purpose Pulsatile delivery of proteins, in which release occurs over a short time after a period of little or no release, is desirable for many applications. This paper investigates the effect of biodegradable polymer shell thickness on pulsatile protein release from biodegradable polymer microcapsules.

Methods Using precision particle fabrication (PPF) technology, monodisperse microcapsules were fabricated encapsulating bovine serum albumin (BSA) in a liquid core surrounded by a drug-free poly(lactide-*co*-glycolide) (PLG) shell of uniform, controlled thickness from 14 to 19 μm.

Results When using high molecular weight PLG (Mw 88 kDa), microparticles exhibited the desired core-shell structure with high BSA loading and encapsulation efficiency (55–65%). These particles exhibited very slow release of BSA for several weeks followed by rapid release of 80–90% of the encapsulated BSA within 7 days. Importantly, with increasing shell thickness the starting time of the pulsatile release could be controlled from 25 to 35 days.

Conclusions Biodegradable polymer microcapsules with precisely controlled shell thickness provide pulsatile release with enhanced control of release profiles.

Electronic supplementary material The online version of this article (doi:10.1007/s11095-014-1412-5) contains supplementary material, which is available to authorized users.

Y. Xia
Department of Chemical and Biomolecular Engineering, University of Illinois, 600 S. Mathews Avenue, Urbana, Illinois 61801, USA

D. W. Pack
Department of Chemical and Materials Engineering, University of Kentucky, 159 F. Paul Anderson Tower, Lexington Kentucky 40506-0046, USA

D. W. Pack (✉)
Department of Pharmaceutical Sciences, University of Kentucky, 467 Biological Pharmaceutical Bldg., 789 S. Limestone, Lexington Kentucky 40536-0596, USA
e-mail: dan.pack@uky.edu

KEY WORDS bovine serum albumin · controlled release · monodisperse microcapsules · poly(lactide-*co*-glycolide) · pulsatile release

INTRODUCTION

Protein therapeutics are being intensively studied in the biotechnology and pharmaceutical industries as promising replacements for traditional small-molecule drugs due to their unique structure, high pharmacological potency, highly specific functions and relatively low side effects [1, 2]. Because proteins are typically fragile, have very short half-lives *in vivo*, and exhibit poor bioavailability, however, frequent injection or infusion is needed. The limited administration route as well as poor control of delivery rates have become major obstacles for the wide application of protein therapeutics [3]. In response, research in advanced protein delivery systems seeks to provide simple, safe and effective methods for administration with control of delivery rates.

Polymer delivery systems, especially biodegradable polymer microparticles, are a popular and promising drug delivery method for therapeutic proteins. Polymer microparticles are relatively easy to fabricate, can be administered via simple injection, and can provide drug release over time periods up to several months [4]. By adjusting size distribution as well as structure of microparticles, researchers were able to tailor protein release rates [5, 6]. Double-wall microspheres or microcapsules composed of two distinct materials with either core-shell or reservoir structure and drug located in one or both of the phases, have been developed for advanced protein or drug delivery [7–16]. These particles usually exhibit extended protein release rates compared to traditional monolithic microspheres. However, there is growing evidence that continuous delivery may not be optimal for all protein drugs; pulsatile delivery is preferred in many cases [17–19]. Pulsatile release is the rapid release of therapeutic during a relatively

short time window after a period of no or slow release [17, 20]. This naturally occurring mechanism has been mimicked for the development of pulsatile protein release systems to improve therapeutic efficacy.

Methods to trigger the pulsatile release include self-degradation/erosion [21], electric fields [22], magnetic fields [23], exposure to ultrasound or light [24], changes in pH or temperature [25] and sophisticated microchip-based devices [26]. Among these, liquid-core biodegradable microparticle systems are relatively simple to fabricate and do not require an exterior stimulus. With therapeutics loaded within liquid cores and surrounded by biodegradable polymer shells, the particle rupture rate and the drug release can be controlled by the properties of the polymers as well as structure of the microcapsules [27–29]. However, due to the relatively broad distribution of particle size and polymer shell thickness, the pulsatile release profiles are usually irregular and often difficult to control [30]. In this study, we report the first example of monodisperse microcapsules composed of a protein-containing liquid core and uniform poly(lactide-*co*-glycolide) (PLG) shell as release rate-controlling layer using precision particle fabrication technique (PPF) [28, 31].

MATERIALS AND METHODS

Materials

Poly(D,L-lactide-*co*-glycolide) (PLG, Mw 15 kDa, 38 kDa and 88 kDa; lactide: glycolide 50:50) were purchased from LACTEL Absorbable Polymers. Chromatography grade dichloromethane (DCM) was obtained from Sigma-Aldrich. Bovine serum albumin (BSA, Mw 66,700 Da) and dimethyl sulfoxide (DMSO) were purchased from Fisher Scientific. Poly(vinyl alcohol) (PVA, Mw 25,000 Da, 88% hydrolyzed) was purchased from Polysciences. Tween 80 was purchased from Acros Organics. Canola oil was purchased from Spectrum Naturals. Bicinchoninic acid (BCA) protein assay reagent was obtained from Pierce.

Liquid-Core Microcapsules Fabrication

A triple nozzle system was employed for producing liquid-core microcapsules using PPF (Supplementary Information Fig. S1). A 23-guage steel hypodermic needle (PrecisionGlide, Becton Dickinson Co.) with flat tip was used as the innermost nozzle, which was surrounded coaxially by the inner glass nozzle (1.5 mm OD, 0.84 mm ID) made from a glass capillary (World Precision Instrument, Inc.). The outer glass nozzle (2.5 mm OD, 1.5 mm ID) surrounded the inner glass nozzle and was made of Pyrex glass (Kimax).

BSA (100 mg/mL in deionized water) was emulsified with canola oil at a volumetric ratio of 1:3 (aqueous:organic) by sonication (CE Converter 102 C, Branson) in an ice-water bath at 50% amplitude for 1 min with a 15 s interval in the middle to form the core phase. The shell phase was 10%*w/v* PLG dissolved in DCM. PVA water solution (0.5%*w/v*) was used as non-solvent carrier stream.

The core phase BSA/canola oil emulsion passed through the innermost metal nozzle and the shell PLG solution passed through the concentric inner glass nozzle. The outermost glass nozzle was for PVA non-solvent carrier stream. The frequency generator (Agilent 33220A) and piezoelectric transducer (CV 33, Sonic & Materials Inc.) generated an acoustic wave on the nozzle system to break the exiting streams into uniform droplets. Nascent microcapsules were collected in 500 mL of 0.5% PVA solution and were stirred for 1 h to allow for DCM extraction and evaporation. The particles were filtered (Filter Paper #4, Whatman), washed three times with deionized water, and lyophilized for 48 h. Samples were stored until use in a −20°C freezer with desiccant.

Particle Size Distribution

The size distributions of nascent particles (wet particles before lyophilizing) were determined using a Coulter Multisizer III (Beckman Coulter Inc.) with a 200 μm aperture in Isoton II. More than 5,000 particles were measured for each sample.

Initial Core Engulfment

Initial core engulfment efficiencies (i.e., the percentage of particles exhibiting cores completely surrounded by shell PLG) were determined for each microparticle sample using light microscopy (Invertoskop, Zeiss). Optical micrographs of several hundred microparticles were captured for each sample at the particle midline. Visual observation was used to determine the number of particles with fully encapsulated cores relative to the total number of particles imaged. All particles exhibiting partial engulfment, for which the core is either protruding from or contacting the exterior wall of the shell, have been treated as not encapsulated.

Protein Loading

Samples of approximately 10 mg of microcapsules were dissolved in 100 μL DMSO. The solution was pipetted into 1 mL of phosphate-buffered saline (PBS, pH 7.4±0.05) then incubated for 1 h at 37°C with shaking at 240 rpm. The mixture was centrifuged for 10 min at 10,000 rpm, and BSA concentration in the supernatant was determined using bicinchoninic acid (BCA) assay. All absorbance measurements were taken on a SpectraMax 340 PC reader equipped with SoFTMax Pro software. The loading equaled the mass of BSA per mass of particles. The encapsulation efficiency equaled the actual

BSA loading divided by theoretical BSA loading multiplied by 100.

In Vitro BSA Release

For each batch of microcapsules, a sample of approximately 30 mg was suspended in 1.25 mL release buffer consisting of 0.05% (*v*/*v*) Tween 80 (to prevent particle agglomeration) and PBS, pH 7.4. These samples were incubated at 37°C with shaking (240 rpm). At various time points, 1.0 mL supernatant was removed and replaced with fresh media in order to maintain constant pH sink condition. Blank microcapsules (same fabrication parameters, except no protein was added) were treated the same way and the supernatants at various time points were collected as controls. The release study was performed in triplicate, and BSA concentrations in the collected supernatants were measured using BCA assay (Pierce) with absorbance corrected by absorbance of supernatants from blank microcapsules.

Scanning Electron Microscopy (SEM)

Microcapsules were prepared for imaging by placing a droplet of an aqueous particle suspension on a silicon stub. The samples were dried overnight and sputter coated with gold and platinum prior to imaging. In order to image the cross-sections, microparticles were frozen in liquid nitrogen and fractured using a razor blade on a glass slide, resuspended in a water droplet, and mounted on silicon stubs. The JEOL 6060 LV scanning electron microscope was used at an acceleration voltage of 3–15 kV.

Particle Degradation/Erosion Study

For each batch of microcapsules, a sample of approximately 5 mg was suspended in 1.25 mL release buffer consisting of 0.05% (*v*/*v*) Tween 80 and PBS. These samples were incubated at 37°C with shaking (240 rpm). As in the release experiment, the buffer was replaced periodically to maintain constant pH. At various time points, all supernatant was removed and the samples were frozen and lyophilized for at least 48 h. The samples were prepared for SEM as described above.

SDS-PAGE

BSA in supernatants during *in vitro* release was subjected to non-reduced sodium dodecyl sulfate polyacrylamide gel electrophoresis (SDS-PAGE) using precast gradient gels (4–20% Tris–HCl/glycine) and Mini-PROTEAN II system (Bio-Rad Laboratories, Inc.). Running buffer (25 mM Tris, 192 mM glycine and 0.1% (*w*/*v*) SDS, pH 8.3) was diluted from 10x Tris/Glycine/SDS buffer. Samples were diluted 1:1 in Laemmli sample buffer (62.5 mM Tris–HCl, pH 6.8, 25% glycerol, 2% SDS, 0.01% Bromophenol blue) under non-reducing conditions (without β-mercaptoethanol or DTT), and heated for 1 min at 95°C prior to loading. Gels were electrophoresed for 40 min at 200 V and then stained with Coomassie blue to visualize the protein bands.

RESULTS

Production of Monodisperse BSA-Loaded Liquid-Core Microcapsules

We investigated the effects of PLG molecular weight (15 kDa, 38 kDa and 88 kDa) on particle fabrication and BSA encapsulation. By changing PLG shell-phase flow rates while keeping the liquid core-phase flow rate constant, we were able to fabricate BSA-loaded liquid-core microcapsules with different shell thickness. Based on the measured diameter of microcapsules as well as monolithic microspheres, PLG shell thickness can be calculated (Table I and Supplementary Information). The calculated liquid core diameter was constant at 45–46 μm, and the shell thickness of PLG increased from ~14 μm to ~19 μm upon increasing the PLG shell phase flow rate from 30 mL/h to 50 mL/h.

Core engulfment was evaluated for each batch of liquid-core microcapsules by transmitted light microscopy (Fig. 1). For lower PLG molecular weight (15 kDa), liquid-core engulfment efficiencies were low (11, 7 and 4%), and many of the microparticles exhibited "acorn"-shape structures with liquid cores protruding at one side. For PLG molecular weight 38 kDa, liquid-core engulfment efficiencies were higher (36, 49 and 17%), but the majority of microparticles were not fully encapsulated. When PLG molecular weight was increased to 88 kDa, high core engulfment efficiencies were achieved (97, 93 and 91%). With one exception (38 kDa PLG, flow rate 40 mL/h), core engulfment efficiency decreased with increasing PLG shell flow rate (Table II).

Protein Loading and Encapsulation Efficiency of Liquid-Core Microcapsules

Initial protein loading and encapsulation efficiency were measured after extracting BSA from the particles (Fig. 2). The BSA loading and encapsulation efficiency decreased as PLG shell flow rates increased from 30 mL/h to 50 mL/h except for the sample with PLG Mw 38 kDa and shell flow rate 40 mL/h, which is in accordance with core engulfment efficiency. In addition, lower PLG molecular weight led to lower loading and encapsulation efficiency. When PLG molecular weight increased to 88 kDa, most of the BSA-loaded liquid cores were fully surrounded by the polymer shell (Table II) and the BSA encapsulation efficiencies reached 55–65%.

Table I Dimensions of Monolithic Microspheres (MS) and Liquid-Core Microcapsules (MC)

Sample	PLG Mw (kDa)	PLG flow rate (mL/h)	Outer diameter, measured (μm)	Core diameter, calculated (μm)	Shell thickness, calculated (μm)
MS	15	30	68.2	N/A[a]	N/A
MS	15	40	73.0	N/A	N/A
MS	15	50	78.4	N/A	N/A
MC	15	30	74.8	46.7	14.1
MC	15	40	78.8	46.4	16.2
MC	15	50	83.0	45.0	19.0
MS	38	30	66.9	N/A	N/A
MS	38	40	73.2	N/A	N/A
MS	38	50	78.6	N/A	N/A
MC	38	30	73.4	45.9	13.8
MC	38	40	79.0	46.4	16.3
MC	38	50	83.4	45.7	18.9
MS	88	30	69.0	N/A	N/A
MS	88	40	74.1	N/A	N/A
MS	88	50	80.0	N/A	N/A
MC	88	30	75.1	45.6	14.7
MC	88	40	79.9	46.9	16.5
MC	88	50	84.6	46.6	19.0

[a] N/A, not applicable

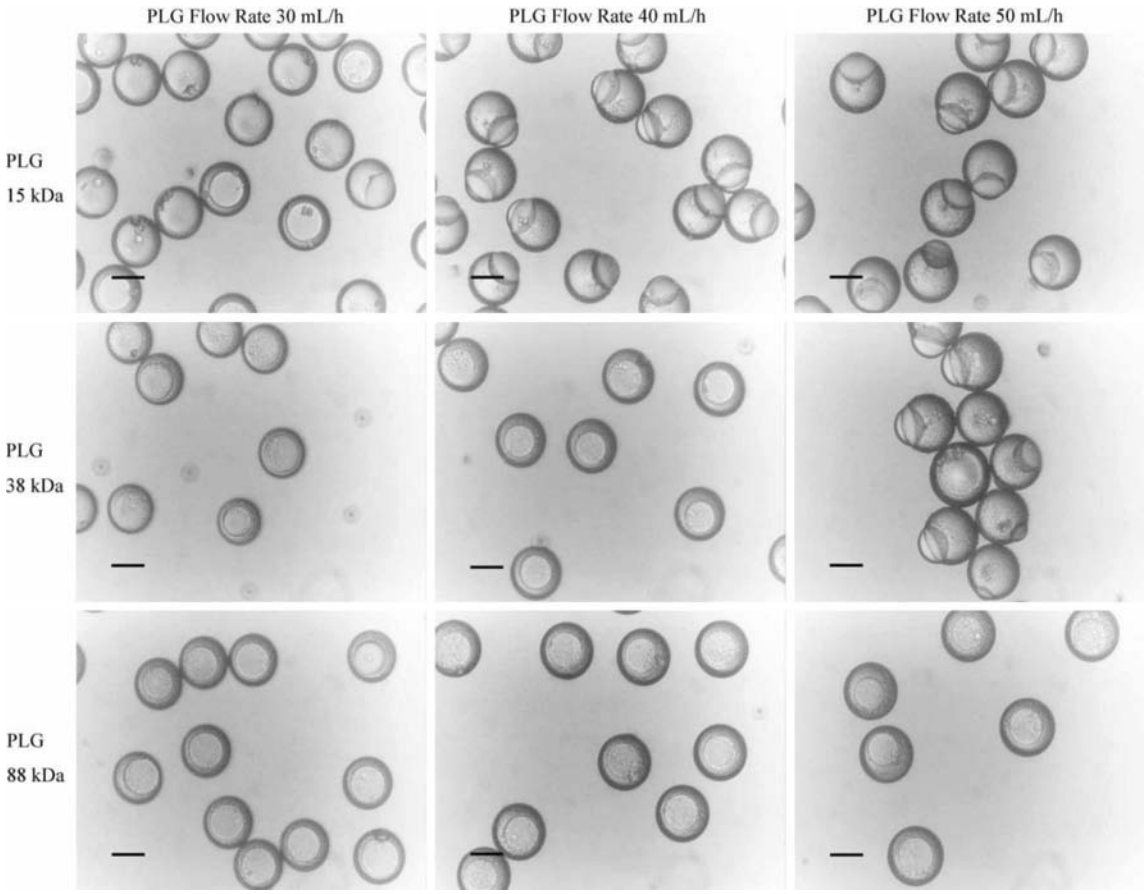

Fig. 1 Transmitted light microcopy of microcapsules with different PLG molecular weight (15, 38 and 88 kDa) and PLG shell flow rates (30, 40 and 50 mL/h). Scale bar = 50 μm.

Table II Microcapsule Core Engulfment Efficiency (%) ± Standard Deviation

	PLG flow rate (mL/h)		
	30	40	50
PLG Mw 15 kDa	11 ± 4	7 ± 3	4 ± 2
PLG Mw 38 kDa	36 ± 6	49 ± 8	17 ± 5
PLG Mw 88 kDa	97 ± 3	93 ± 2	91 ± 3

BSA *in Vitro* Release

BSA release profiles were obtained relative to the measured protein loading of liquid-core microcapsules (Fig. 3). The final amount released reached 100–115%, most likely due to under-estimation of the initial loading caused by incomplete extraction of BSA from the microcapsules.

For 15 kDa PLG, the liquid-core engulfment efficiencies (4–11%, Table II), BSA loading, and encapsulation efficiency (Fig. 2) were low. Most of the liquid cores containing BSA were either protruding from one side of the particles or attached on the surface of microparticles. The corresponding BSA release rates were very fast, and complete BSA release was reached at ~10 days (Fig. 3a).

For 38 kDa PLG, with PLG shell flow rates of 30 and 40 mL/h, the liquid-core engulfment efficiencies were 36 and 49%, respectively. BSA release rates were relatively fast from day 1 to day 10, probably due to the microparticles with the liquid cores not fully encapsulated. Subsequently, release rates decreased, and complete BSA release was observed at ~40 days. For PLG flow rates of 50 mL/h, the liquid-core engulfment efficiency was only 17%, and fast BSA release was observed, similar to microparticles with 15 kDa PLG, with complete BSA release at ~20 days (Fig. 3b).

Microparticles with higher PLG molecular weight (Mw 88 kDa) achieved high liquid core engulfment efficiencies (91–97%, Table II). The BSA release profiles were very different compared to microparticles containing lower

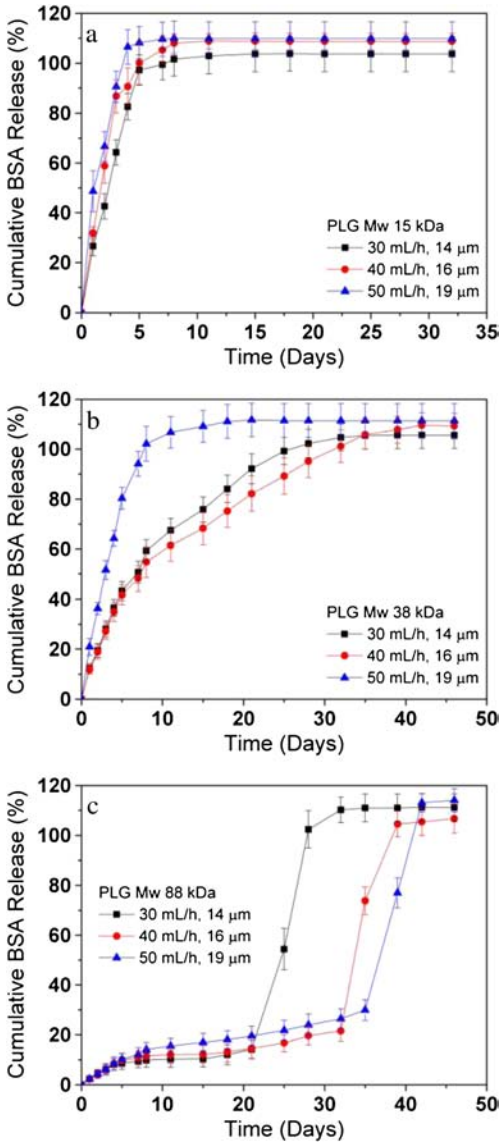

Fig. 3 *In vitro* release profiles of liquid-core microcapsules of different PLG molecular weight ((**a**), 15 kDa; (**b**), 38 kDa; (**c**), 88 kDa) with different PLG shell flow rate (30, 40 and 50 mL/h) and calculated shell thickness (~14, 16 and 19 μm).

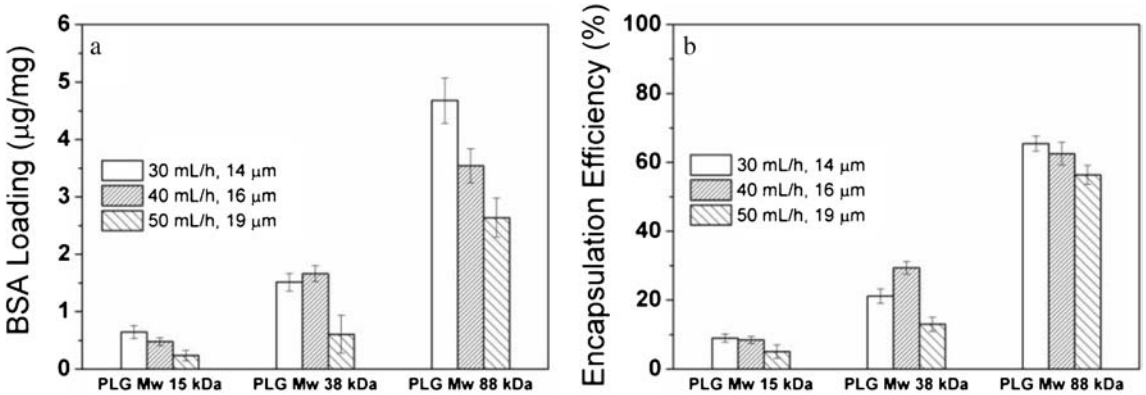

Fig. 2 Microcapsule loading (**a**) and encapsulation efficiencies (**b**) of different PLG molecular weight (15, 38 and 88 kDa) with PLG shell flow rates (30, 40 and 50 mL/h) and corresponding calculated PLG shell thickness (~14, 16 and 19 μm).

molecular weight PLG. For PLG shell flow rates 30 mL/h (calculated shell thickness 14.7 μm, Table I), only ~10% BSA was released in the first ~20 days. From day 25 to day 32, the remainder of the BSA was released. For PLG shell flow rates 40 mL/h (calculated shell thickness 16.5 μm, Table I), ~20% of encapsulated BSA was released by 32 days, and a BSA burst release was observed from day 32 to day 40. For PLG shell flow rates 50 mL/h (calculated shell thickness 19.0 μm, Table I), similarly, ~25% of BSA was slowly released by day 35, followed by rapid, complete release of BSA at day ~42 (Fig. 3c).

Surface and Interior Morphology of Liquid-Core Microcapsules

Scanning electron microscopy was employed to study the initial morphology of the microparticle surface and interior. For core-shell microcapsules, cross-section micrographs were obtained, while for the poorly formed microparticles, only higher magnification micrographs of the particle surfaces were obtained (Fig. 4, Fig. S3).

For microcapsules with lower PLG molecular weight (15, 38 kDa), microparticles were clearly not spherical; only the solid remainder of the acorn-shape particles was observed. For 15 kDa PLG, porous structures were observed on the surface for PLG shell flow rate 30 mL/h, while increasing PLG shell flow rate to 40 and 50 mL/h, the surfaces became relatively smooth. For 38 kDa PLG, wrinkles appeared on the surfaces of all microparticles. Upon increasing PLG molecular weight to 88 kDa, spherical microparticles were observed. Porous structures and wrinkles appeared on the surface of these microcapsules, and the cross-section micrographs revealed core-shell structures (Fig. 4).

Liquid-Core Microcapsules Morphology During *in Vitro* Degradation/Erosion

To better understand the degradation and erosion of the liquid-core microcapsules and to correlate BSA with release profiles, microcapsules (PLG Mw 88 kDa, PLG shell flow rate 30, 40 and 50 mL/h) were imaged by SEM at various times during the release experiment (Fig. 5).

For microcapsules with PLG shell flow rate 30 mL/h (calculated shell thickness 14.7 μm), surface porosity increased from day 10 to day 20, and at day 30 microcapsules had collapsed. These results were in accordance with the *in vitro* BSA release profile in which most of the protein was released from day 25 to 32. For microcapsules with PLG flow rates 40 mL/h and 50 mL/h, similarly, surface porosity increased before particles broke into pieces between 30 and 40 days. These results also agreed with *in vitro* release profiles in which these two batches of microcapsules showed a pulsatile release from days ~32–40 and days ~35–42, respectively.

BSA Stability During *in Vitro* Release

BSA in supernatants from the *in vitro* release was examined using SDS-PAGE as a measure of stability of the released protein. No reducing agent such as β-mercaptoethanol or DTT was used, to preserve any disulfide-linked protein aggregates. BSA may undergo

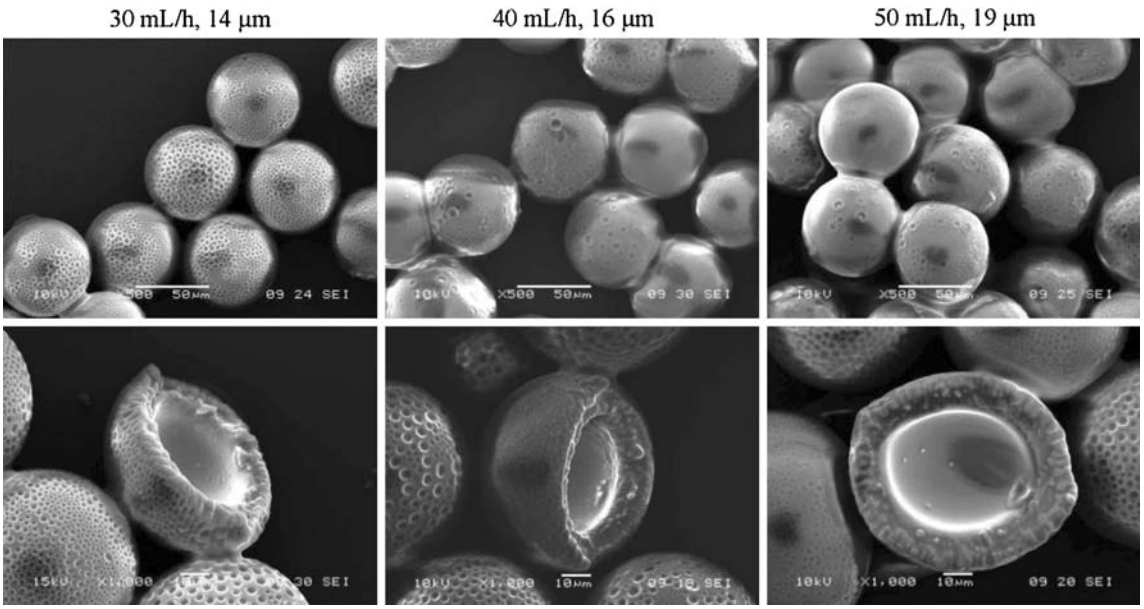

Fig. 4 SEM images of microcapsules of PLG molecular weight 88 kDa with PLG shell flow rate (30, 40 and 50 mL/h) and calculated shell thickness (~14, 16 and 19 μm).

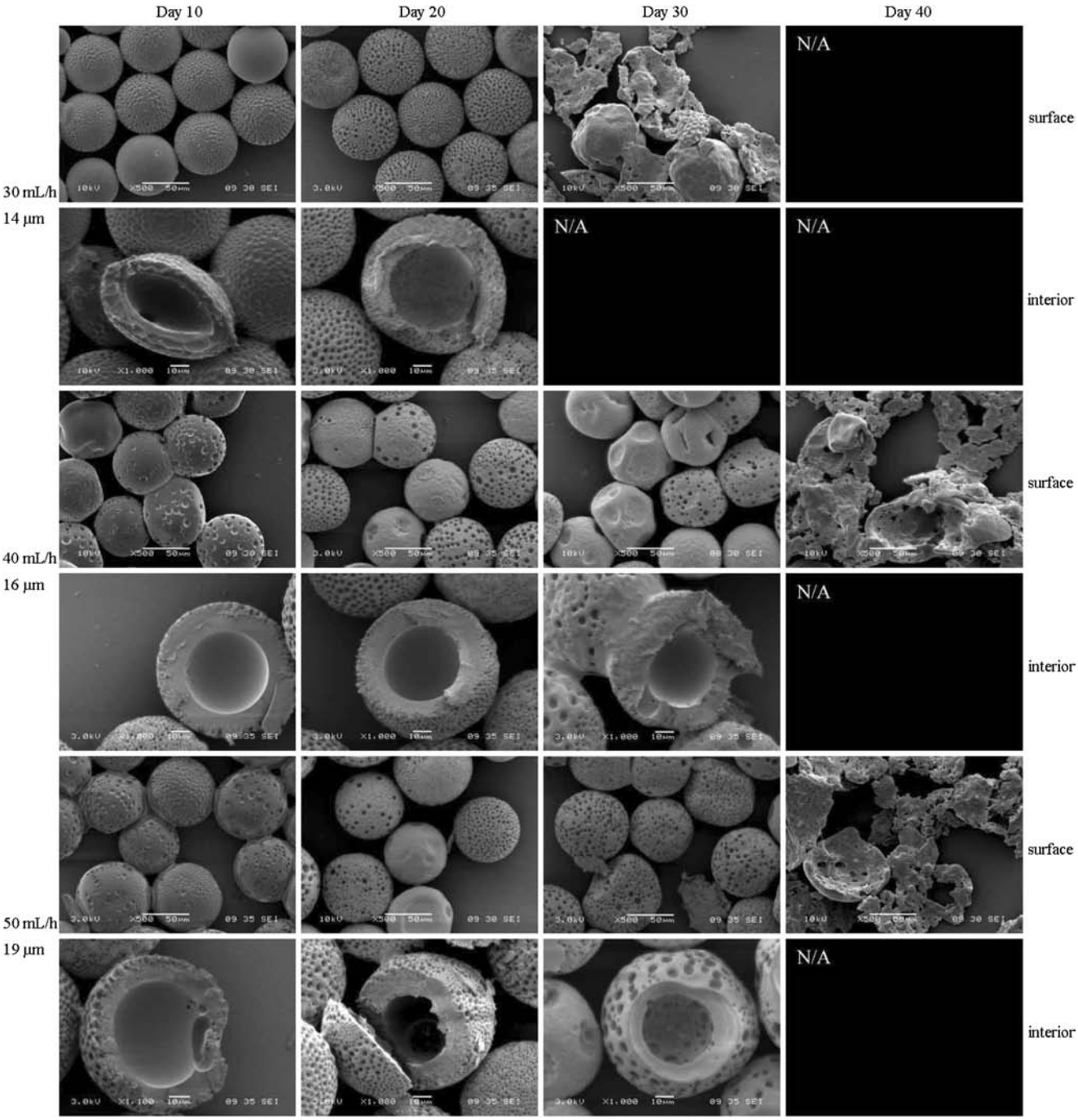

Fig. 5 SEM images of microcapsules degradation/erosion study with different PLG (Mw 88 kDa) shell flow rate (30, 40 and 50 mL/h).

covalent or non-covalent aggregation as well as hydrolysis during matrix degradation and erosion, because BSA may attach to the matrix and the microclimate within the particles may become acidic [32]. Non-reduced SDS-PAGE was performed on samples from days 28, 35 and 39 for 88 kDa microcapsules with PLG shell flow rates of 30, 40 and 50 mL/h, respectively. Primarily BSA monomers (around 60 kDa) were observed with no detectable BSA aggregation or degradation bands revealed (Fig. 6).

DISCUSSION

Biodegradable microparticle size distribution and structure are crucial factors for controlling protein delivery rates. We have produced monodisperse liquid-core microcapsules with core-shell structure using PPF. The fragile liquid cores with encapsulated model protein BSA can be properly confined using biodegradable polymer PLG of high molecular weight.

Fabrication of liquid-core microcapsules is dependent on polymer solution phase (PLG in DCM) fully spreading over

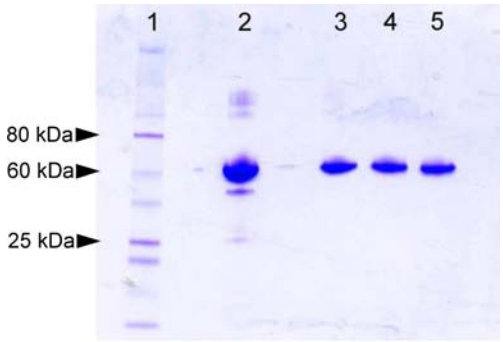

Fig. 6 SDS-PAGE gel of BSA in supernatants of liquid-core PLG (Mw 88 kDa) microcapsules: Lane 1: protein ladder (10–250 kDa); lane 2: fresh BSA solution; lane 3: BSA from liquid-core microcapsules with PLG shell flow rate 30 mL/h at Day 28; lane 4: BSA from liquid-core microcapsules with PLG shell flow rate 40 mL/h at day 35; lane 5: BSA from liquid-core microcapsules with PLG shell flow rate 50 mL/h at day 39.

the liquid-core phase (emulsion of canola oil and BSA water solution). The engulfment is described by spreading coefficient theory as developed by Harkins [33]. Torza and Mason extended Harkin's theory to systems of two immiscible phases suspended in a third immiscible phase [34]. Equation (1) allows calculation of the spreading coefficient for each phase from the interfacial tensions between the phases: γ_{12}, γ_{23} and γ_{13}.

$$\lambda_{ij} = \gamma_{jk} - \gamma_{ij} - \gamma_{ik} \tag{1}$$

Since $\gamma_{ij}=\gamma_{ji}$, there are only three independent spreading coefficients defining the system, and these can be referred to by their first subscript:

$$\begin{aligned} \lambda_1 &= \lambda_{12} = \lambda_{13} \\ \lambda_2 &= \lambda_{23} = \lambda_{21} \\ \lambda_3 &= \lambda_{31} = \lambda_{32} \end{aligned} \tag{2}$$

Assuming phase 2 is the suspending PVA phase and phase 1 (liquid core) is specified to be such that $\gamma_{12}>\gamma_{32}$ (i.e. $\lambda_1<0$), it is found that only three possible scenarios exist for the values of the spreading coefficients in Table III. Case A is total engulfment of liquid core by PLG solution phase (phase 3), Case B is partial engulfment, and Case C is no engulfment (Fig. 7). By Harkins' definition, a positive spreading coefficient leads to spreading. In Case A, total engulfment will occur

Table III Prediction of Final Configuration Based on Spreading Coefficients

Case A	Case B	Case C
$\lambda_1<0$	$\lambda_1<0$	$\lambda_1<0$
$\lambda_2<0$	$\lambda_2<0$	$\lambda_2>0$
$\lambda_3>0$	$\lambda_3<0$	$\lambda_3<0$

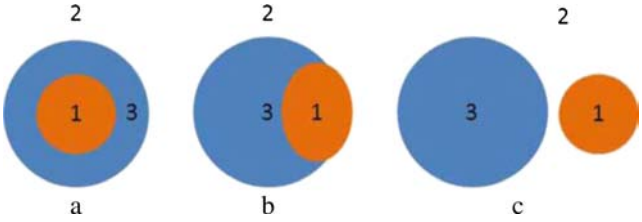

Fig. 7 Schematic of possible liquid phase and PLG phase spreading configurations: (**a**) total engulfment (*core-shell microcapsules*), (**b**) partial engulfment (*acorn-shape*) and (**c**) no engulfment.

since λ_3 is positive, i.e. PLG phase wants to spread on liquid core. For Case B, since all spreading coefficients are negative, none of the phases wants to spread on any of the others, and a three component line interface results (acorn-shape structure). When spreading coefficient 1 and 3 are negative but 2 is positive, a separate phase system is present. In this case the solvent PVA wants to spread around both liquid core and PLG shell.

Interfacial tension is commonly approximated as $\gamma_{ij} = \left(\sqrt{\gamma_i} - \sqrt{\gamma_j}\right)^2$ [35], where γ_i is the liquid/air surface tension. For PLG, PVA and liquid-core emulsion, the exact γ_i is unknown. Since polymer surface tension increases with molecular weight [36], interfacial tension of PLG/PVA (γ_{32}) as well as interfacial tension of PLG/liquid core (γ_{31}) can either increase (if $\sqrt{\gamma_3} > \sqrt{\gamma_2}$, $\sqrt{\gamma_3} > \sqrt{\gamma_1}$) or decrease (if $\sqrt{\gamma_3} < \sqrt{\gamma_2}$, $\sqrt{\gamma_3} < \sqrt{\gamma_1}$) with molecular weight. Thus, the sum of $\gamma_{31}+\gamma_{32}$ can also increase or decrease with increasing PLG molecular weight. For lower PLG molecular weight (15, 38 kDa), acorn-shape microparticles comprised a large percentage of the particles, so Case B appears to have occurred and $\lambda_3=\gamma_{12}-\gamma_{31}-\gamma_{32}=\gamma_{12}-(\gamma_{31}+\gamma_{32}) < 0$. Thus, $\gamma_{12}<\gamma_{31}+\gamma_{32}$ (i.e. interfacial tension of liquid-core phase/PVA is smaller than the sum of interfacial tension of PLG solution with the two other phases). Upon increasing PLG molecular weight to 88 kDa, most microparticles are core-shell structure microcapsules, so Case A apparently occurred and $\lambda_3=\gamma_{12}-\gamma_{31}-\gamma_{32}=\gamma_{12}-(\gamma_{31}+\gamma_{32}) > 0$, thus $\gamma_{12}>\gamma_{31}+\gamma_{32}$ (i.e. interfacial tension of liquid-core phase and PVA is bigger than the sum of interfacial tension of PLG with two other phases).

The transmitted light microscopy as well as BSA loading and encapsulation efficiency confirmed that when the PLG fully encapsulated the liquid core forming the core-shell structure, BSA loading and encapsulation efficiency were high. From BSA *in vitro* release profiles, we found that only microcapsules with core-shell structure generated pulsatile or burst release after microparticles were incubated for several weeks. In addition, with increasing PLG shell flow rates and, thus, increasing PLG shell thickness, the starting time of pulsatile release was delayed.

SEM was used to study the initial microparticle morphology and microcapsule morphology during *in vitro* degradation. For 88 kDa PLG microcapsules, core-shell structures were

observed throughout degradation until the microcapsules collapsed. The surfaces became more porous and microcapsules gradually lost spherical shape during degradation. The pulsatile release profiles correlated with the time at which microcapsules ruptured. Throughout degradation, the porous structures probably caused by PLG degradation developed in the PLG shell until the microcapsules ruptured and most BSA was released within a short time.

Only monomeric BSA was observed in the released protein samples. This result contrasts with many reports of protein release from PLG microparticles in which aggregation and proteolysis are often observed [37, 38]. It is well known that the low pH microenvironment within degrading PLG particles, resulting from accumulation of acidic polymer degradation products, plays a major role in the loss of protein stability [39, 40]. We suggest that the unusual stability of released BSA observed in this work was due to loading of BSA in the oil-based core, which may have prevented acidic degradation products from reaching the protein-containing domains within the core. It remains possible, however, that some fraction of the encapsulated BSA was converted to insoluble aggregates that were not released from the particles. Future research will investigate the mechanisms of protein stability within the microcapsules and the stability of any BSA remaining in the particles.

CONCLUSIONS

Monodisperse liquid-core microcapsules with different shell thickness were successfully fabricated using precision particle fabrication by keeping the liquid-core phase flow rate constant while gradually increasing PLG shell flow rate (30 mL/h, 40 mL/h and 50 mL/h). By using higher molecular weight PLG (88 kDa), most microparticles exhibited core-shell structure, and BSA loading and encapsulation efficiency were high. The *in vitro* release profiles of BSA confirmed the hypothesis that BSA pulsatile release could be achieved using liquid-core microcapsules, and increasing microcapsule shell thickness while keeping the protein-loaded liquid core diameter constant postponed the starting time of pulsatile release.

ACKNOWLEDGMENTS

This work was supported by the National Institute of Health Grant EB005181 and GM085222. Scanning Electron Microscopy took place in Material Research Lab at University of Illinois at Urbana-Champaign. Confocal microscopy measurements took place in Beckman Institute, imaging technology group at University of Illinois at Urbana-Champaign. DSC was performed in Microanalysis Laboratory, School of Chemical Sciences, University of Illinois at Urbana-Champaign.

REFERENCES

1. Leader B, Baca QJ, Golan DE. Protein therapeutics: a summary and pharmacological classification. Nat Rev Drug Discov. 2008;7:21–39.
2. Aggarwal S. What's fueling the biotech engine-2009-2010. Nat Biotechnol. 2010;28:1165–71.
3. Ye M, Kim S, Park K. Issues in long-term protein delivery using biodegradable microparticles. J Control Release. 2010;146:241–60.
4. Varde NK, Pack DW. Microspheres for controlled release drug delivery. Expert Opin Biol Ther. 2004;4:35–51.
5. Berkland C, Pollauf E, Raman C, Silverman R, Kim K, Pack DW. Macromolecule release from monodisperse plg microspheres: control of release rates and investigation of release mechanism. J Pharm Sci. 2007;96:1176–91.
6. Xia Y, Xu Q, Wang C-H, Pack DW. Protein encapsulation in and release from monodisperse double-wall polymer microspheres. J Pharm Sci. 2013;102:1601–9.
7. Sato K, Takahashi S, Anzai J-I. Layer-by-layer thin films and microcapsules for biosensors and controlled release. Anal Sci. 2012;28:929–38.
8. Bysell H, Månsson R, Hansson P, Malmsten M. Microgels and microcapsules in peptide and protein drug delivery. Adv Drug Deliv Rev. 2011;63:1172–85.
9. Sawalha H, Schroën K, Boom R. Biodegradable polymeric microcapsules: preparation and properties. Chem Eng J. 2011;169:1–10.
10. Rahman NA, Mathiowitz E. Localization of bovine serum albumin in double-walled microspheres. J Control Release. 2004;94:163–75.
11. Berkland C, Cox A, Kim KK, Pack DW. Three-month, zero-order piroxicam release from monodispersed double-walled microspheres of controlled shell thickness. J Biomed Mater Res. 2004;70A:576–84.
12. Berkland C, Pollauf E, Pack DW, Kim K. Uniform double-walled polymer microspheres of controllable shell thickness. J Control Release. 2004;96:101–11.
13. Berkland C, Pollauf EJ, Varde NK, Pack DW, Kim KK. Monodisperse liquid-filled biodegradable microcapsules. Pharm Res. 2007;24:1007–13.
14. Xia Y, Ribeiro PF, Pack DW. Controlled protein release from monodisperse biodegradable double-wall microspheres of controllable shell thickness. J Control Release. 2013;172:707–14.
15. Xu Q, Xia Y, Wang C-H, Pack DW. Monodisperse double-walled microspheres loaded with chitosan-p53 nanoparticles and doxorubicin for combined gene therapy and chemotherapy. J Control Release. 2012;163:130–5.
16. Xu Q, Leong J, Chua QY, Chi YT, Chow PK-H, Pack DW, *et al.* Combined modality doxorubicin-based chemotherapy and chitosan-mediated p53 gene therapy using double-walled microspheres for treatment of human hepatocellular carcinoma. Biomaterials. 2013;34:5149–62.
17. Roy P, Shahiwala A. Multiparticulate formulation approach to pulsatile drug delivery: current perspectives. J Control Release. 2009;134:74–80.
18. Kikuchi A, Okano T. Pulsatile drug release control using hydrogels. Adv Drug Deliv Rev. 2002;54:53–77.
19. Bussemer T, Otto I, Bodmeier R. Pulsatile drug-delivery systems. Crit Rev Ther Drug Carrier Syst. 2001;18:433–58.
20. Richards Grayson AC, Choi IS, Tyler BM, Wang PP, Brem H, Cima MJ, *et al.* Multi-pulse drug delivery from a resorbable polymeric microchip device. Nat Mater. 2003;2:767–72.
21. Makino K, Mogi T, Ohtake N, Yoshida M, Ando S, Nakajima T, *et al.* Pulsatile drug release from poly (lactide-co-glycolide)

microspheres: how does the composition of the polymer matrices affect the time interval between the initial burst and the pulsatile release of drugs? Colloids Surf B: Biointerfaces. 2000;19:173–9.
22. Yuk S, Cho S, Lee H. Electric current-sensitive drug delivery systems using sodium alginate/polyacrylic acid composites. Pharm Res. 1992;9:955–7.
23. Edelman ER, Kost J, Bobeck H, Langer R. Regulation of drug release from polymer matrices by oscillating magnetic fields. J Biomed Mater Res. 1985;19:67–83.
24. Kost J, Leong K, Langer R. Ultrasound-enhanced polymer degradation and release of incorporated substances. Proc Natl Acad Sci U S A. 1989;86:7663–6.
25. Siegel RA, Falamarzian M, Firestone BA, Moxley BC. Ph-controlled release from hydrophobic/polyelectrolyte copolymer hydrogels. J Control Release. 1988;8:179–82.
26. Santini Jr JT, Cima MJ, Langer R. A controlled-release microchip. Nature. 1999;397:335–8.
27. Bussemer T, Bodmeier R. Formulation parameters affecting the performance of coated gelatin capsules with pulsatile release profiles. Int J Pharm. 2003;267:59–68.
28. Berkland C, Pollauf E, Varde N, Pack DW, Kim KK. Monodisperse liquid-filled biodegradable microcapsules. Pharm Res. 2007;24:1007–13.
29. Sanchez A, Gupta RK, Alonso MJ, Siber GR, Langer R. Pulsed controlled-release system for potential use in vaccine delivery. J Pharm Sci. 1996;85:547–52.
30. Youan BBC, Jackson TL, Dickens L, Hernandez C, Owusu-Ababio G. Protein release profiles and morphology of biodegradable microcapsules containing an oily core. J Control Release. 2001;76:313–26.
31. Berkland C, Kim K, Pack DW. Fabrication of plg microspheres with precisely controlled and monodisperse size distributions. J Control Release. 2001;73:59–74.
32. Fu K, Pack DW, Klibanov AM, Langer R. Visual evidence of acidic environment within degrading poly(lactic-co-glycolic acid) (plga) microspheres. Pharm Res. 2000;17:100–6.
33. Harkins WD, editor. The physical chemistry of surface films. New York: Reinhold; 1952.
34. Torza S, Mason SG. Three-phase interactions in shear and electrical fields. J Colloids Int Sci. 1970;33:67–83.
35. van Krevelen DW, editor. Properties of polymers: Their estimation and correlation with chemical structure. Amsterdam: Elsevier Scientific Publishing Company; 1976.
36. Anastasiadis SH, Gancarz I, Koberstein JT. Interfacial tension of immiscible polymer blends: temperature and molecular weight dependence. Macromolecules. 1988;21:2980–7.
37. Schwendeman SP. Recent advances in the stabilization of proteins encapsulated in injectable plga delivery systems. Crit Rev Ther Drug Carrier Syst. 2002;19:26.
38. Emami J, Hamishehkar H, Najafabadi AR, Gilani K, Minaiyan M, Mahdavi H, *et al.* A novel approach to prepare insulin-loaded poly(lactic-co-glycolic acid) microcapsules and the protein stability study. J Pharm Sci. 2009;98:1712–31.
39. Houchin ML, Topp EM. Chemical degradation of peptides and proteins in plga: a review of reactions and mechanisms. J Pharm Sci. 2008;97:2395–404.
40. Fredenberg S, Wahlgren M, Reslow M, Axelsson A. The mechanisms of drug release in poly(lactic-co-glycolic acid)-based drug delivery systems—a review. Int J Pharm. 2011;415:34–52.